

Evaluating the seismic performance of a structure founded on liquefiable soil at the Port of Wellington during the 2013 and 2016 New Zealand earthquakes

Jonathan D. Bray
 University of California-Berkeley, Berkeley, USA

William Z. Zakka
 University of California-Berkeley, Berkeley, USA

ABSTRACT: The 2016 M_w 7.8 Kaikōura earthquake caused widespread liquefaction-induced damage at the Port of Wellington, New Zealand. Conversely, less intense, shorter duration ground shaking during the 2013 M_w 6.6 Cook Strait and Lake Grassmere earthquakes caused no-to-moderate damage. The PM4Sand, PM4Silt, and UBCHyst constitutive models implemented in the FLAC8.1 software are used to back-analyze the available well-documented field case histories. Nonlinear effective stress seismic site response analyses are performed to calculate the ground shaking at a strong motion site at the Port. The analytical results agree with the recorded ground motions. The same motions and models are employed in two-dimensional nonlinear effective stress dynamic analyses of the 2-story CPH reinforced concrete frame structure with spread footings at the Port during the three earthquakes to investigate its performance. No-to-minor damage was documented at the CPH building site during the 2013 earthquakes, but the ground and structure settled relatively uniformly approximately 230-260 mm in the 2016 Kaikōura earthquake. The analyses reliably captured the observed structural response during the earthquakes. Negligible settlement was estimated for the 2013 earthquakes, and the volumetric-induced liquefaction mechanism governed the seismic performance of the structure in the 2016 Kaikōura earthquake with only minor shear-induced settlement. Shear-induced settlement was minor due to the light weight of the structure and the strength of the 3-m thick compacted gravelly fill crust. A recently developed simplified procedure provided results reasonably consistent with these analyses.

KEYWORDS: Analysis, dynamic, earthquake, foundation, liquefaction, performance, structure.

1 INTRODUCTION

Reclaimed fills are commonly used to construct critical ports, yet they are susceptible to liquefaction and the resulting effects of liquefaction. Ground shaking during the 2016 M_w 7.8 Kaikōura earthquake triggered significant liquefaction at the Port of Wellington (CentrePort), New Zealand. The port was damaged significantly, and operations were suspended following the earthquake (Cubrinovski et al. 2017). Previous lower intensity and shorter duration ground shaking from the 2013 Cook Strait and Lake Grassmere earthquakes (both M_w 6.6) caused negligible damage or localized moderate damage. There is merit to examine the performance of the port and its facilities during these three earthquakes to evaluate the suitability of the design procedures commonly employed in engineering practice. Intensity measures of the recorded ground motions during the three earthquakes at the CPLB strong motion station (SMS) at CentrePort are provided in Table 1.

Table 1. Intensity measures of recorded ground motions at CPLB strong motion station for the three earthquakes.

Earthquake	PGA ¹ (g)	S _a (1s) ¹ (g)	I _a ¹ (m/s)	D ₅₋₉₅ ¹ (s)	CAV _{STD} ¹ (g-s)
2016 Kaikōura	0.24	0.47	1.71	24.8	1.18
2013 Lake Grassmere	0.14	0.26	0.28	11.6	0.23
2013 Cook Strait	0.22	0.45	0.55	10.1	0.40

¹PGA = peak ground acceleration, S_a(1s) = spectral acceleration at 1 s period, I_a = Arias intensity, D₅₋₉₅ = significant duration, and CAV_{STD} = standardized cumulative absolute velocity. All intensity measures correspond to the median single-component horizontal ground motion across all non-redundant azimuths (RotD50).

Liquefaction triggering and its effects are often evaluated using simplified procedures (e.g., Boulanger and Idriss 2014, Zhang et al. 2002, and Bray and Macedo 2017). Greater insights can be gained through the performance of dynamic nonlinear effective stress analyses. Nonlinear analyses can capture in part the complex response of soil undergoing liquefaction and the interactions of structures and the ground beneath them. Dynamic nonlinear soil-structure interaction (SSI) analyses are especially useful at identifying the governing mechanisms of

liquefaction-induced building settlement and to estimate the shear-induced component of building settlement (e.g., Luque and Bray 2017). Dynamic analyses require the development of input ground motions. One-dimensional (1D) site response analyses are useful to evaluate the appropriateness of input “rock” motions through comparison of the calculated ground surface motions with recorded motions. This study employs two-dimensional (2D) SSI dynamic nonlinear effective stress analyses to investigate liquefaction-induced building settlement features of a two-story structure at CentrePort. The results of these analyses are compared with field observations and the results from simplified procedures. Key insights are shared.

2 SITE CONDITIONS

Wellington is an important port city near the southern tip of New Zealand’s north island. Reclaimed land has enlarged the city and its port facilities. Wellington’s original coastline is about 200 to 500 m inland from its current coastline. Reclamations at CentrePort were constructed between 1882 and 1976 (Figure 1). Reclamations at the north of the port consist of hydraulic fills constructed in 1924 to 1932 using dredged material (sandy and silty soils) from the original seabed. The southern areas of the port were built with gravelly soil from 1882 to 1916 with the Thorndon Reclamation constructed in 1965 to 1976 by end-tipping, in which gravelly soils from nearby quarries were dumped into the sea creating a Gravel-Sand-Silt (G-S-S) soil mixture (Dhakal et al. 2020a). The thickness of the fill varies across the port, increasing with distance from the original coastline. Marine sediment underlies the fill, and the Wellington alluvium beneath it extends to the Greywacke basement rock at a depth of about 115 m. The groundwater table (GWT) is 2 m to 3 m deep at the port.

Significant in situ ground characterization data have been collected at Centreport since 2017, including 121 cone penetration tests (CPTs) at the locations shown in Figure 1, shear wave velocity measurements, and 33 soil borings with laboratory tests (Dhakal et al. 2020a, Vantassel et al. 2018). Five CPTs were conducted near the CPLB SMS that was in the pre-1916 gravelly soil reclamation shown in Figure 1.

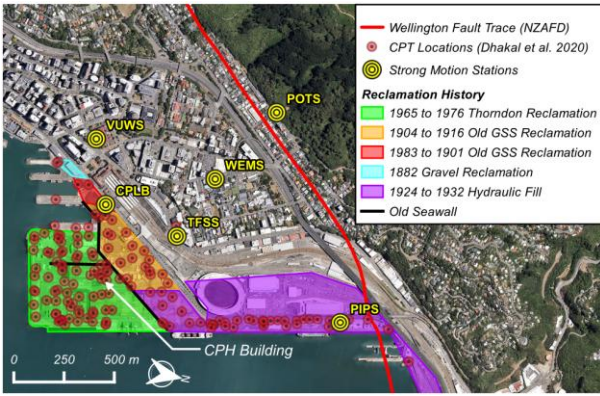


Figure 1. Map of CentrePort showing location of CPH building, strong motion stations, and CPT locations (CPT data from Dhakal et al. 2020; base image from Google Earth 2024).

The CPTs near the CPLB SMS are used to characterize the subsurface conditions to develop input ground motions at this site. Analyses are conducted using two representative profiles from CPTu032 and SCPTu096 to consider spatial variability in the CPT readings. CPT readings for the SCPTu096 profile up to a depth of 4 m are combined with data from CPT030 because it was predrilled to this depth. Shear-wave velocity (V_s) was measured near the CPLB SMS using multi-channel analysis of surface waves (MASW). They form the basis of the interpreted V_s profile. Direct push cross-hole V_s measurements are used to refine the top 25 m of the profile. The interpreted SCPTu096 soil profile is shown in Figure 2. Results presented in this paper correspond to this profile. The CPTu032 profile produced comparable results.

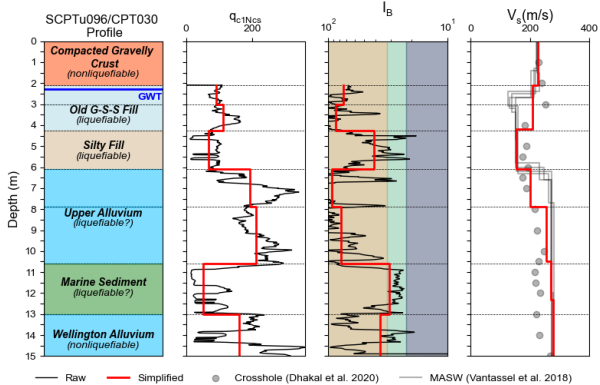


Figure 2. A representative soil profile at the CPLB SMS based on SCPTu096/CPT030 with normalized tip resistance q_{c1NCS} (using Boulanger and Idriss 2014), modified soil behavior type index I_B (using Robertson 2016), and shear wave velocity V_s (Vantassel et al. 2018).

3 INPUT GROUND MOTIONS

CentrePort is at the edge of the Thorndon Basin. This large basin structure affects the ground response at CentrePort. Dhakal et al. (2022) analyzed the use of outcropping motions, as well as deconvolved motions from the SMS in Wellington and concluded the deconvolved motions from the VUWS SMS (shown in Figure 1) were the most adequate for site response analysis at CentrePort. Deconvolved surface motions are used instead of outcropping rock motions because the surface motions incorporate basin edge effects that are not present at the rock site. Deconvolution of the surface motions preserves some of these basin edge features present in the recordings and leads to improved forward analysis. This approach compensates for the fact that these 3D effects cannot be explicitly captured using 1D methods. Deconvolution has been used commonly to back-analyze field case histories (e.g., Markham et al. 2015).

Independently deconvolved input motions from this study are similar to the motions developed by Dhakal et al. (2022). The two horizontal components of the recorded ground motions for the three earthquakes at the VUWS SMS are deconvolved to the greywacke bedrock ($V_s = 1200$ m/s) using the equivalent-linear 1D STRATA program (Kottke and Rathje 2009). The shear modulus reduction and material damping curves are based on Darendeli (2001) and Menq (2003).

Fully coupled 1D nonlinear effective stress seismic site response analyses are conducted using FLAC v8.1 (Itasca 2019) to ensure the earthquake ground motions recorded at the CPLB SMS could be captured. Fully coupled nonlinear effective stress analyses are preferred at this site because liquefaction manifestations were observed near the CPLB SMS. The 1D soil column was composed of quadratic elements extending from a depth of 115 m (i.e., greywacke bedrock) to the ground surface. The lateral boundaries of the soil column are attached to simulate simple shear type deformation in free-field level-ground conditions. The elements are 0.3 m to 1 m thick to ensure accurate wave propagation (Kuhlemeyer and Lysmer 1973). The compliant base layer is modelled using an elastic element with quiet boundary conditions that absorb reflected waves using two sets of dashpots attached independently to the mesh in the normal and shear directions following the recommendations of Lysmer and Kuhlemeyer (1969). Ground motions are applied to the compliant base as shear stress-time histories following the procedure recommended by Mejia and Dawson (2006). The analyses are conducted using both horizontal orthogonal ground motions (North-South and East-West directions) for each of the three major earthquakes.

The 5%-damped RotD50 acceleration response spectra of the deconvolved bedrock horizontal motions from the VUWS SMS for the 2013 Cook Strait and 2016 Kaikoura earthquakes are shown with the black solid lines in Figure 3. The 5%-damped acceleration response spectra of the calculated RotD50 horizontal ground motions at the ground surface are compared with the acceleration response spectra of the RotD50 motions recorded at the CPLB SMS for the 2013 Cook Strait and 2016 Kaikoura earthquakes (shown in solid color lines and dashed gray lines, respectively in Fig. 3). The computed and recorded response spectra match well for these two events as well as for the 2013 Lake Grassmere earthquake (not shown). Hence, the deconvolved input bedrock motions and the model of the site conditions at CentrePort are judged to be reasonable. Additional details on the development of input motions and the seismic site response study are provided in Zakka and Bray (2025).

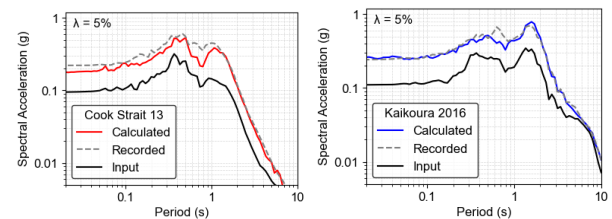


Figure 3. Comparison of 5%-damped elastic acceleration response spectra of calculated and recorded RotD50 horizontal ground motions at CPLB for the 2013 Cook Strait and 2016 Kaikoura earthquakes, with deconvolved input bedrock motions from the VUWS SMS.

4 NUMERICAL ANALYSES OF CPH BUILDING

4.1 CPH building

The CPH building was located at S41.278 E174.786 until it was demolished after the 2016 Kaikoura earthquake. The CPH building was a reinforced concrete (RC) frame structure founded on RC spread footings connected with tie beams. The building was 78.5 m in length in the E-W direction and 16 to 17

m wide in the N-S direction. It was composed of two connected building sections: a 2-story office structure comprised most of the building with a 3-story control structure located on its east side, which included an additional story of a light steel frame. The structures shared a common foundation, and its two sections were separated by a 50-mm thick seismic gap. The height of the building was about 7.4 m and 10 m for the office section and the control section of the CPH building, respectively. This study focuses on the response of the office building section as it is more representative of the dynamic response of the entire CPH building.

Figure 4 shows the foundation plan of the CPH building and a typical NS-oriented structural frame for the office part of the building. The exterior building footing width (B) is 1.4 m with an estimated footing bearing pressure (Q) of 50 kPa based on 100% of the structural dead loads and 20% of the design live loads. Alternatively, considering the entire building footprint due to its tie beams and underlying stiff gravel, its width (B) is 16 m with an estimated building pressure (Q) of 12 kPa. The structure's fundamental period is estimated to be around 0.2 s. The locations of 8 CPTs performed around the building are shown in Figure 4.

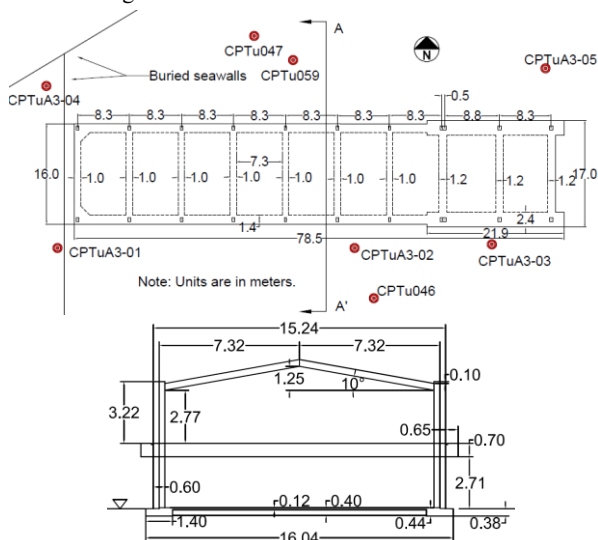


Figure 4. Plan view of the foundation of the CPH building with surrounding CPTs and a typical structural frame (section A-A') of the office section of the building.

4.2 CPH building performance

Liquefaction-induced building settlement mechanisms can be categorized as shear-induced, volumetric-induced, and ejecta-induced (Bray and Olaya 2023). Sediment ejecta were not observed near the CPH building during the 2013 Cook Strait, 2013 Lake Grassmere, and 2016 Kaikōura earthquakes. Thus, the ejecta-induced component of liquefaction building settlement is negligible (i.e., 0), and it is not considered further in this assessment. Hutabarat and Bray (2022) CPT-based procedure estimates no ejecta for the 2013 Lake Grassmere earthquake, but overestimates ejecta as being severe for the 2013 Cook Strait and 2016 Kaikōura earthquakes.

The Bray and Olaya (2023) CPT-based procedure is used to estimate the volumetric-induced component of building settlement based on all surrounding CPTs shown in Figure 4. It is estimated as the 1D free-field level ground settlement of the Thorndon dumped gravelly soil reclamation. The volumetric-induced component of the building/ground settlement at the CPH building site for the 2013 Cook Strait and 2016 Kaikōura earthquakes are provided in Tables 2 and 3. Ground settlement at the CPH building site was measured relative to the ground

supported on old, buried bulk heads of the Pipitea Wharf west of the building that did not appear to settle.

The volumetric-induced ground settlement is estimated at the 16% to 84% exceedance levels to be 15 to 50 mm and 60 to 180 mm for the 2013 Lake Grassmere and 2013 Cook Strait earthquakes, respectively. Measured ground settlement of 10 – 40 mm near the CPH building after the 2013 Lake Grassmere Earthquake aligns with the estimated range. Ground following the 2013 Cook Strait was not surveyed but is estimated to have settled less than 100 mm (Dhakal et al. 2020b). Liquefaction volumetric-induced ground settlement is estimated to be 100 mm to 290 mm for the constructed fill for the 2016 Kaikōura earthquake. This estimate is consistent with the measured ground settlement of 180 mm to 260 mm considering the complexity of the liquefaction-induced ground settlement phenomenon. Thus, the volumetric-induced settlement is estimated reliably with the Bray and Olaya (2023) procedure for the large and low intensity events but is slightly overestimated for the moderate Cook Strait event. Another simplified procedure (Zhang et al. 2002) performed similarly in another liquefaction assessment study at the port during the 2013 and 2016 earthquakes (Dhakal et al. 2020b).

The Bray and Macedo (2017) CPT-procedure is employed to estimate the shear-induced component of building settlement for the earthquakes affecting CentrePort using all surrounding CPTs. The depth of the foundation (D_f) is 0.4 m. The geometric mean thickness of the liquefied layers (H_L) is 4.4 m and 7.0 m and the geometric mean liquefaction building settlement (LBS) parameter for the foundation of the CPH building is 14 and 23 for the 2013 Cook Strait and 2016 Kaikōura earthquakes, respectively.

These values of LBS and H_L are used with the two sets of the building parameters of $B = 1.4$ m and $Q = 50$ kPa and $B = 16$ m and $Q = 12$ kPa to develop an average estimate of the building settlement for an intermediate foundation response. The earthquake ground shaking demand parameters are cumulative absolute velocity (CAV_{STD}) of 0.40 g^*s and 1.18 g^*s and a spectral acceleration at 1 second (Sa_1) of 0.45 g and 0.47 g for the 2013 Cook Strait and 2016 Kaikōura earthquakes, respectively (both are RotD50 values). While the procedure recommends using CAV_{dp} for forward-analyses, the use of CAV_{STD} for back-analysis to capture the median response of a case history where ground motions records exist is preferable. Additionally, CAV_{dp} and CAV_{STD} are similar for these grounds motions and yield equivalent estimates. The 16% to 84% shear-induced component of liquefaction building settlement is estimated to be negligible-to-minor for the 2013 Cook Strait earthquake, which is consistent with observations. The 16% to 84% shear-induced component of liquefaction building settlement is estimated to be 20 mm to 50 mm for the 2016 Kaikōura earthquake, which is consistent with the observed shear-induced building settlement of 0 mm to 50 mm.

Table 2. Building settlement for 2013 Cook Strait earthquake

Type of settlement	Measured ¹ (mm)	Estimated (mm)
Volumetric-induced settlement	<100	60 - 180
Shear-induced settlement	-	0 - 20
Total settlement	<100	60 - 200

¹Estimated by Dhakal et al. (2020b). Ground near CPH was not surveyed after the Cook Strait event.

Table 3. Building settlement for 2016 Kaikōura earthquake

Type of settlement	Measured (mm)	Estimated (mm)
Volumetric-induced settlement	180 - 260	100 - 290
Shear-induced settlement	0 - 50	20 - 50
Total settlement	230-260	120 - 340

In summary, there was negligible-to-minor evidence of liquefaction and ground settlement at the CPH site with no structural damage of the CPH building following the 2013 Cook Strait and Lake Grassmere earthquakes. Conversely, the CPH building and the surrounding fill settled relatively uniformly 230-260 mm during the 2016 Kaikoura earthquake. Significant structural damage was not observed following this event. The nearly uniform settlement of the CPH building that was consistent with the uniform ground settlement at the site for the 2016 Kaikoura earthquake indicates the governing mechanism is the volumetric-induced component of liquefaction building settlement. The shear-induced component of liquefaction building settlement is relatively minor. It is informative to perform advanced nonlinear analyses of this case history of relatively uniform building/ground settlement, because most of the cases examined by Bray and Macedo (2017) included a significant amount of shear-induced building settlement.

4.3 Finite difference model

Fully coupled 2D nonlinear effective stress dynamic analyses of the CPH building and its site are performed using FLAC v8.1 (Itasca 2019). The finite difference method model is shown in Figure 5. As was done in the 1D analyses, element heights are selected to ensure accurate wave propagation and lateral boundaries with nodes attached in the horizontal direction are placed sufficiently far from the structure to minimize their influence and capture free-field conditions. In the 2D model, the compliant base is set at a depth of 50 m using elastic elements.

The input ground motions for nonlinear 2D dynamic analyses are developed using the deconvolved input bedrock motions described previously. The greywacke bedrock ($V_s = 1200$ m/s) motions at depth of 115 m are propagated up to a depth of 50 m within the Wellington alluvium ($V_s = 350$ m/s) using the equivalent-linear method in STRATA (Kottke and Rathje 2009). These ground motions are then applied at the compliant base of the 2D model as a shear stress time history following the recommendations of Mejia and Dawson (2006).

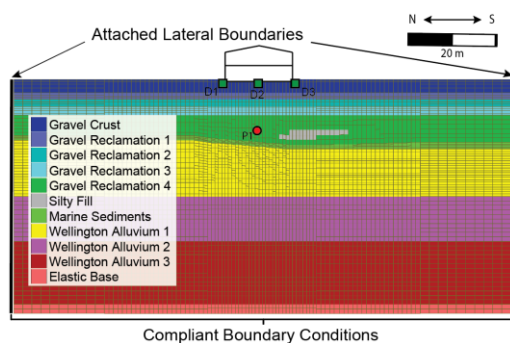


Figure 5. Finite difference mesh of analysis of CPH building.

Liquefiable gravel reclamation is modelled using PM4Sand v3.3 (Boulanger and Ziotopoulou 2023). The silty fill and marine sediments layers are modelled using PM4Silt v2.1 (Boulanger and Ziotopoulou 2022). PM4Sand and PM4Silt are stress-ratio controlled critical state-based bounding surface plasticity models capable of simulating the contractive-dilatative response of sand and capturing the cyclic softening of plastic materials, respectively. The UBCHyst model developed by Naesgaard (2011) is used to model the compacted gravelly crust and the Wellington alluvium, because significant generation of excess pore water pressure is not expected in these materials. UBCHyst is a total stress model developed for nonliquefiable soils based on the Mohr-Coulomb model that is capable of simulating shear modulus reduction and hysteretic damping.

The non-default parameters for the PM4Sand, PM4Silt, and UBCHyst models are listed in Table 4 and Table 5, respectively. Soil parameters are estimated primarily using CPT data following a similar procedure as described in Zalka and Bray (2025). Small-strain shear moduli are estimated using V_s measurements at the site (Vantassel et al. 2018). The PM4Sand contraction rate parameter (h_{p0}) is calibrated to match the target cyclic resistance ratio (CRR) estimated using the Boulanger and Idriss (2014) CPT-based procedure. Similarly, the cyclic resistance in PM4Silt is calibrated to match empirical curves from Boulanger and Idriss (2007). Default values are used for secondary parameters in PM4Sand and PM4Silt. Shear modulus reduction and material damping of soil units modelled with UBCHyst are calibrated to match the curves in Menq (2003) and Darendeli (2001) for the gravel crust and alluvium, respectively. The crust D_{50} particle size and coefficient of uniformity (C_u) are estimated to be 5 mm and 80, respectively, based on data provided in Rhodes et al. (2019). Plasticity index of the alluvium is estimated to be 16 based on laboratory tests (Dhakal et al. 2020a), and the layer is assumed to be normally consolidated. Additional Rayleigh damping of 0.5% centered at 0.8 Hz was added to the model for numerical stability.

Table 4. PM4Sand and PM4Silt model parameters.

Layer	Model	Mean q_{clNcs}	Dr (%)	$\frac{S_{u,eq,cs}}{\sigma'_{vc}}$	G_0	h_{p0}	k (m/s)
Gravel Rec.	PM4Sand	87	52	-	1126-1533	0.24-0.29	1.3E-6
Silty Fill	PM4Silt	55	-	0.84	1498	45	9.1E-8
Marine Sed.	PM4Silt	14	-	0.59	1298	50	1.5E-8

Table 5. UBCHyst model parameters.

Layer	G (MPa)	K (MPa)	ϕ' (deg)	c' (kPa)	n	R_f	k (m/s)
Gravel Crust	198	517	54	0	1.4	1.0	7.4E-6
Wellington All.	177-204	451-531	40	0	1.25	1.0	7.4E-6

The structural frame is modelled using linear beam elements with an elastic Young's modulus (E) and RC unit weight of concrete of 2.35E7 kPa and 24 kN/m³, respectively. Flexural cracking of the tie beams was considered by applying a factor of 0.35 their moment of inertia (ACI 318-19). The mass distribution in the out-of-plane direction was addressed by using a typical frame spacing of 8.3 m.

4.4 Numerical Results

The ejecta-induced component of liquefaction-induced building settlement cannot be estimated directly using FLAC v8.1 and the constitutive models currently available. Hence, dynamic analyses are not employed to assess this mechanism. Additionally, the volumetric component of building settlement is most reliably estimated using empirical based approaches instead of the finite difference method (Bray and Olaya 2023). The 1D free-field liquefaction-induced ground settlement method used previously to estimate this component of liquefaction-induced building settlement will be used again in this assessment. Fully coupled 2D nonlinear effective stress dynamic analysis using FLAC v8.1 and the PM4Sand, PM4Silt, and UBCHyst constitutive models are ideally suited for evaluating the shear-induced component of liquefaction building settlement. It is the focus of the numerical analyses.

Results from the nonlinear dynamic analysis are compared with the previously estimated and measured settlements. Analyses were terminated at the end of strong shaking; thus, they do not include most of the post-liquefaction volumetric reconsolidation settlement that occurs due to the dissipation of excess pore water pressures. The numerical results are comparable with the estimated shear-induced liquefaction building settlement component listed in Tables 2 and 3.

Seismic response profiles in terms of the peak ground acceleration (PGA), maximum excess pore water pressure ratio (r_{u-max}), and maximum (engineering) shear strain (γ_{max}) directly below the CPH building for the three earthquakes are shown in Figure 6. The seismic demand and response are the largest during 2016 Kaikōura earthquake, followed by the 2013 Cook Strait earthquake, and finally the 2013 Lake Grassmere earthquake. During the Kaikōura earthquake, liquefaction is expected to be triggered in the Thorndon gravel reclamation with the calculated r_{u-max} reaching 1.0 over much of the reclamation thickness. The calculated maximum shear strain exceeds 3%. Liquefaction is not estimated to trigger during the 2013 events, and large shear strains are not estimated to develop. These results are consistent with observations during the three events.

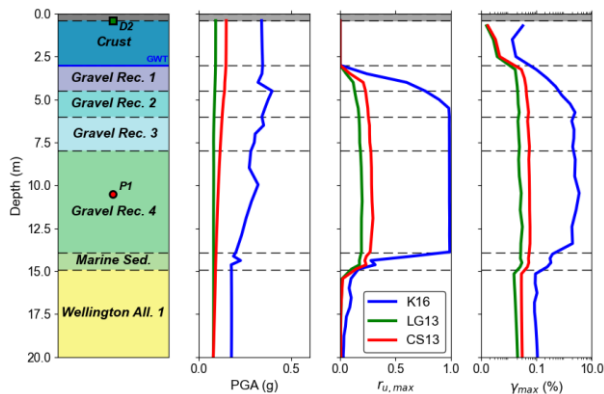


Figure 6. Seismic response profiles below the CPH Building during the three earthquakes: K16 – Kaikōura, LG13 – Lake Grassmere, and CS13 – Cook Strait from the 2D analyses.

Figure 7 shows the accumulation of shear-induced building settlement (D_s) with the generation of excess water pressure and the acceleration-time histories at the center of the building foundation and the input motion at the base of the model for the 2013 Cook Strait and 2016 Kaikōura earthquakes. As shown in Figure 7a, the excess pore water pressure ratio (r_u) during the 2013 Cook Strait earthquake reaches a maximum of about 30% in the liquefiable gravel reclamation and does not trigger liquefaction. In contrast, as shown in Figure 7b, r_u exceeds 98% and liquefaction is triggered during the 2016 Kaikōura earthquake, which is consistent with observations.

Similarly, vertical settlement of the structure commences when r_u approaches unity and liquefaction is triggered in the gravel reclamation. The results of the numerical simulations provide a reasonable explanation of the measured shear-induced liquefaction settlement of the CPH building following the 2016 Kaikōura. Shear-induced building settlement was not measured after the 2013 Cook Strait earthquakes, but it is believed to be negligible. The Bray and Macedo (2017) simplified procedure for estimating shear-induced liquefaction building settlement is in reasonable agreement with the numerical results for the intense 2016 Kaikōura earthquake and the less intense 2013 Cook Strait earthquake.

5 CONCLUSIONS

The liquefaction-induced building settlement of the 2-story shallow-founded CPH structure at CentrePort during the 2013 Cook Strait earthquake and 2016 Kaikōura earthquake is captured using fully coupled 2D dynamic nonlinear effective stress analysis with FLAC v8.1 and the PM4Sand, PM4Silt, and UBCHyst constitutive models. CPT, V_s , and borehole data enabled the constitutive models to be calibrated. The results of nonlinear effective stress seismic site response analyses agreed

with the recorded ground motions, which provided confidence that the deconvolved input bedrock motions were realistic.

Shear-induced liquefaction building settlement was not observed at the CPH building site during the 2013 earthquake, which is consistent with the negligible settlement calculated in the dynamic analyses. The observed shear-induced liquefaction building settlement was minor (i.e., $D_s = 0 - 50$ mm) during the 2016 Kaikōura earthquake, which is consistent with the shear-induced building settlement of 30 mm to 45 mm calculated in the dynamic analyses. Thus, the dynamic nonlinear effective stress analyses captured the shear-induced component of liquefaction settlement of the CPH building for the 2013 Cook Strait earthquake that produced negligible settlement and for the 2016 Kaikōura earthquake that produced minor building settlement. Shear-induced settlement was negligible or minor during these earthquakes largely due to the light weight of the structure and the strength of the 3-m thick compacted gravelly fill crust.

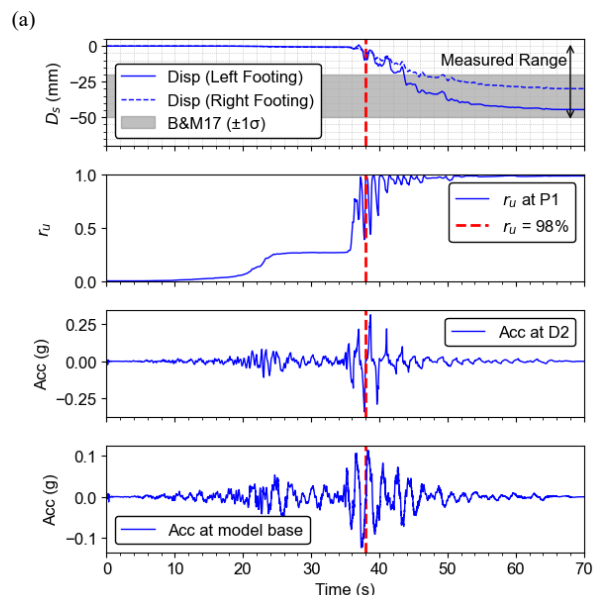
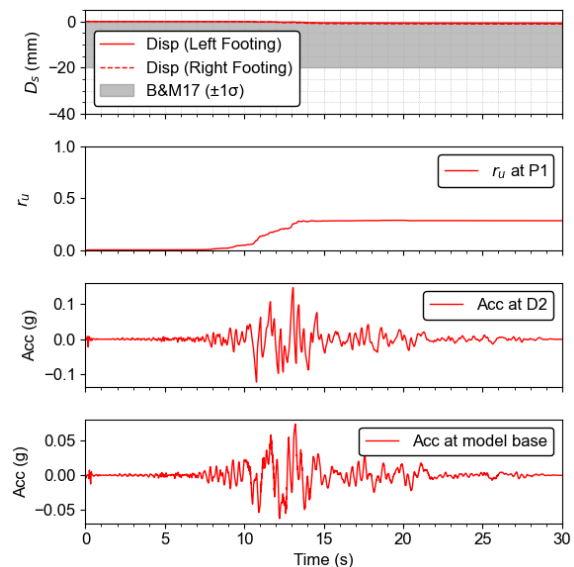


Figure 7. 2D analysis calculated shear-induced settlement-time histories of the CPH building for the: (a) 2013 Cook Strait earthquake and (b) 2016 Kaikōura earthquake. Measured range of building settlement shown for the 2016 Kaikōura event. Locations of P1 and D2 are shown in Fig. 5.

Liquefaction did induce volumetric settlement at the CPH building site during the 2016 Kaikōura earthquake. The ground settled uniformly approximately 180 - 260 mm due to volumetric settlement in this event. Liquefaction volumetric-induced ground settlement was estimated to be 100 - 290 mm for the gravel fill for the 2016 Kaikōura earthquake using the Bray and Olaya (2023) procedure, which is reasonably consistent with the observed 1D ground settlement. The volumetric component of building settlement governed the performance of the structure during the 2016 Kaikōura earthquake. The structure was not damaged significantly by the relatively uniform ground and foundation settlement.

Negligible-to-minor ground settlement was observed during the 2013 earthquakes, which is captured well by the Bray and Olaya (2023) procedure for the low intensity Lake Grasmere earthquake, but it is overestimated slightly by this procedure for the moderate intensity Cook Strait earthquake. Additionally, the ejecta-induced settlement is overestimated by the Hutabarat and Bray (2022) procedure for the Cook Strait and Kaikōura earthquakes, although it captures the lack of ejecta-induced settlement for the Lake Grasmere earthquake. Studies of additional field case histories are warranted to examine these issues further.

6 ACKNOWLEDGEMENTS

This work is supported in part by the National Science Foundation (NSF) through the Engineering for Civil Infrastructure Program under grant CMMI-1956248 and the graduate research fellowship program (GRFP). Any opinions, findings, conclusions, or recommendations expressed in this material are those of the authors and do not necessarily reflect the views of the NSF. The authors thank Prof. Misko Cubrinovski and Dr. Riway Dhakal of the University of Canterbury for their collaboration. The authors also thank Jeff Silverwood of CentrePort Ltd for providing access to building plans.

7 REFERENCES

ACI Committee 318. 2019. *Building Code Requirements for Structural Concrete (ACI 318-19) and Commentary (ACI 318R-19)*. American Concrete Institute.

Boulanger, R. W., and Idriss, I. M. 2007. Evaluation of cyclic softening in silts and clays. *J. Geotech. Geoenviron. Eng.*, 133(6), 641-652.

Boulanger, R. W., and Idriss, I. M. 2014. CPT and SPT Based Liquefaction Triggering Procedures." Report No. UCD/CGM-14/01. *Center for Geotechnical Modeling, Dept. of Civil and Environmental Engineering*, University of California, Davis.

Boulanger, R. W., and Ziotopoulou, K. 2023. PM4Sand (Version 3.3): A sand plasticity model for earthquake engineering applications. Report No. UCD/CGM-23/01, *Center for Geotechnical Modeling, Department of Civil and Environmental Engineering*, University of California, Davis, CA.

Boulanger, R. W., and Ziotopoulou, K. 2022. PM4Silt (Version 2): A silt plasticity model for earthquake engineering applications. Report No. UCD/CGM-22/03, *Center for Geotechnical Modeling*, University of California, Davis, CA.

Bray, J.D., and Olaya, F.R. 2023. 2022 H. Bolton Seed Memorial Lecture: Evaluating Liquefaction Effects. *J Geotech Geoenviron Eng.*, ASCE, V. 149(8), doi: 10.1061/JGGEFK.GTENG-11242.

Bray, J. D., and Macedo, J. 2017. 6th Ishihara lecture: Simplified procedure for estimating liquefaction-induced building settlement. *Soil Dynamics and Earthquake Engineering*, 102, 215-231.

Cubrinovski, M., Bray, J. D., de la Torre, C., Olsen, M., Bradley, B. A., Chiaro, G., Stocks, E., and Wotherspoon, L. 2017. Liquefaction effects and associated damages observed at the Wellington CentrePort from the 2016 Kaikōura Earthquake. *Bull. N. Z. Soc. Earthq. Eng.*, 50(2), 152-173.

Darendeli, M. B. 2001. *Development of a new family of normalized modulus reduction curves and material damping curves*. Ph.D. dissertation, Dept. of Civil Eng., Univ. of Texas, Austin.

Dhakal, R., Cubrinovski, M., & Bray, J. D. 2020a. Geotechnical characterization and liquefaction evaluation of gravelly reclamations and hydraulic fills (Port of Wellington, New Zealand). *Soils and Foundations*, 60(6), 1507-1531.

Dhakal, R., Cubrinovski, M., and Bray, J. D. 2020b. Liquefaction Assessment of Reclaimed Land at CentrePort, Wellington. *Bull. N. Z. Soc. Earthq. Eng.*, 53(1), 1-12.

Dhakal, R., Cubrinovski, M., and Bray, J. D. 2022. Input Ground Motion Selection for Site Response Analysis at the Port of Wellington (New Zealand). *Geotechnical, Geological and Earthquake Engineering*, 52, Springer, Cham. https://doi.org/10.1007/978-3-031-11898-2_64.

Hutabarat, D., and Bray J.D. 2022. Estimating the Severity of Liquefaction Ejecta using the Cone Penetration Test. *J. of Geotechnical and Geoenvironmental Engineering*, ASCE, V. 148(3), 10.1061/(ASCE)GT.1943-5606.0002744.

Itasca. 2019. *FLAC, Fast Lagrangian Analysis of Continua, User's Guide, Version 8.1*. Itasca Consulting Group, Inc., Minneapolis, MN.

Kottke, A. R., and Rathje, E. M. 2009. *Technical manual for Strata*. Pacific Earthquake Engineering Research Center, Berkeley, CA.

Kuhlemeyer, R. L., and Lysmer, J. 1973. Finite element method accuracy for wave propagation problems. *J. Soil Mech. Found. Div.*, 99(5), 421-427.

Luque, R., and Bray, J. D. 2017. Dynamic analyses of two buildings founded on liquefiable soils during the Canterbury earthquake sequence. *J. Geotech. Geoenviron. Eng.*, 143(9), 04017067.

Lysmer, J., and Kuhlemeyer, R. L. 1969. Finite dynamic model for infinite media. *J. Eng. Mech. Div.*, 95(4), 859-877.

Markham, C.S., Bray, J.D. and Macedo, J. 2015. Deconvolution of surface motions from the Canterbury Earthquake Sequence for Use in Nonlinear Effective Stress Site Response Analyses. *Proceedings of the 6th International Conference on Earthquake Geotechnical Engineering* (Vol. 176).

Mejia, L. H., and Dawson, E. M. 2006. Earthquake Deconvolution for FLAC. *Proc., 4th Int. FLAC Symp.*, Madrid, Spain.

Menq, F. Y. 2003. *Dynamic properties of sandy and gravelly soils*. Ph.D. dissertation, Dept. of Civil Eng., Univ. of Texas, Austin.

Naesgaard, E. 2011. A hybrid effective stress-total stress procedure for analyzing embankments subjected to potential liquefaction and flow. Ph.D. thesis, Civil Engineering Department, The University of British Columbia, Vancouver, B.C.

Rhodes, A., Keepa, C., Cubrinovski, M., & Krall, T. (2019). Liquefaction evaluation of gravelly reclamation fill at CentrePort, Wellington. *Earthquake Geotechnical Engineering for Protection and Development of Environment and Constructions*.

Robertson, P. K. 2016. Cone penetration test (CPT)-based soil behaviour type (SBT) classification system—an update. *Can. Geotech. J.*, 53(12), 1910-1927.

Vantassel, J., Cox, B., Wotherspoon, L., and Stolte, A. 2018. Deep shearwave velocity profiling and fundamental site period measurements at CentrePort, Wellington. *Bull. Seismol. Soc. Am.*, 108(3). <https://doi.org/10.1785/0120170287>.

Zakka, W.Z. and Bray, J.D. 2025. Nonlinear Effective Stress Site Response Analyses of Liquefiable Soils at the Port of Wellington. *Geo-Extreme 2025*, accepted.

Zhang, G., Robertson, P. K., and Brachman, R. W. I. 2002. Estimating Liquefaction Induced Ground Settlements from CPT for Level Ground. *Can. Geotech. J.*, 39(5), 1168-1180